Synthesis and Characterization of Magnetic Nanocomposites of Fullerene-Containing Polyurethane Films for Microwave Applications

Swati Chopra, Mritunjay Kr. Pandey, Sarfaraz Alam

Defence Materials Stores Research and Development Establishment, DMSRDE, Kanpur, Uttar Pradesh, India

Received 28 January 2010; accepted 15 August 2010
DOI 10.1002/app.33195
Published online 11 February 2011 in Wiley Online Library (wileyonlinelibrary.com).

ABSTRACT: Novel nanocomposites of barium hexaferrite- and fullerene-containing polyurethane were synthesized and characterized by scanning electron microscopy, transmission electron microscopy, X-ray diffractometry, and energy-dispersive X-ray diffraction. The nanoparticles showed good dispersion in the polyurethane matrix. Their thermal, mechanical, and electromagnetic absorbance properties were studied. The complex permeability and permittivity were measured in the frequency range of 8.2–12.4 GHz. The maximum reflection loss of the nanocomposites was found to increase with increasing the ferrite content from 1% to 5%, with maximum value of −7.5 dB at only 5% composition. The incorporation of nanofiller not only imparts mechanical strength to the nanocomposite but also shows good radar-absorbing properties at only 5% filler concentration. © 2011 Wiley Periodicals, Inc. J Appl Polym Sci 120: 3204–3211, 2011

Key words: fullerene; polyurethane; nanocomposite; ferrite; TEM; electromagnetic absorbing

INTRODUCTION

The increasing innovatory industrial sector of electronic materials, especially in the telecommunication area, currently applies large-scale equipment that emits radiation in the microwave band in man's daily life. Microwave absorbers are in use since long, both in civil and military applications on account of their ability to eliminate electromagnetic wave pollution and to reduce radar signatures. It is a specially designed material to suppress the reflected electromagnetic energy incident on the surface of the absorber by dissipating the magnetic and electrical components of the wave into heat. The dissipation occurs when the microwave infiltrating the structure of absorber is attenuated by lossy characteristics of the absorber.[1] Recently, the demand for various kinds of microwave absorbers has increased in the frequency range of 1–20 GHz, because of their twofold use, electromagnetic interference shielding and countermeasure to radar detection. Microwave absorbers from ferrite-related materials used in a high frequency such as X band have been particularly noticed.[2–5] These radar-absorbing materials, based on ferrites, have been extensively investigated for their potential application in military fields.

Conventional spinel-type ferrites do not function well in the GHz range because of a drop in the complex permeability as given by Snoek's limit.[6] Content added to obtain required permeability values comprise over 70–80% weight of the filler, inducing critical problems in terms of weight and efficiency. Compared with the ferrites with spinel and garnet structure, hexagonal barium ferrites can be used as good microwave absorber in the frequency range of 1 to more than 20 GHz because of their high saturation magnetization, unusually large coercivity, excellent chemical stability, corrosion resistance, and adjustable anisotropy through ion doping.[7–9] $BaFe_{12}O_{19}$ (BaFe), a well known permanent magnet having a magnetoplumbite-type structure (hexagonal) with fairly large crystal anisotropy along C-axis, has attracted an extensive attention for the last few decades.[10,11] However, ferromagnetic materials have a serious defect plaguing microwave absorbers applications, namely eddy current losses.[12] Suppression of these losses can be accomplished by reducing their size to smaller than the skin depth and by physically isolating them with nonconductive polymer resin and rubber materials. Hence, nanometer-sized ferrite, which show rich magnetic properties depending on the surface anisotropy and chemical composition, such as superparamagnetism[13] and unusual large coercivities,[14] and with strong potential applications to microwave and millimeter-wave components, were chosen for further study. Although metal-doped or -coated barium ferrite composites have been extensively investigated for their hysteresis and

Correspondence to: S. Alam (sarfarazkazmi@yahoo.com).
Contract grant sponsor: DMSRDE; contract grant number: DRM-546.

electromagnetic properties,[15,16] only few researches have studied the microwave absorbing properties of the polymer barium ferrite composites.[17–19]

The incorporation of nanoscale inorganic particles into organic polymers have been widely investigated considering the extra advantages that could be obtained with combined properties of organic materials (mechanical strength and magnetic and thermal stability) and the organic polymers (flexibility, dielectric, ductility, and processibility).[20] The effect of nanobarium titanate on the mechanical, electrical, thermal, morphological, and radar-absorbing properties has been studied on the ferrite filler poly(ether ether ketone) composites by our group.[21–23] Polyurethanes (PUs) are a good choice for organic polymer because of their flexibility and good chemical and corrosion resistance.

The free-standing flexible PU films have been synthesized in our laboratory from fullerenol (hydroxyl fullerene) as a hypercross-linker for synthesizing three-dimensional network of PU.[24] The inorganic filler, BaFe, is expected to impart mechanical and thermal stability in addition to the magnetic properties to the nanocomposite film. For general radar-absorbing material in the form of composite, filler that is effective at a low concentration is always desirable. This is because the strength and ductility of a composite tend to decrease with increasing filler concentration when the filler–matrix bonding is poor. Furthermore, a low filler content is also desirable because of greater processibility, cost saving, and weight saving. In this communication, we study the effect of nanobarium hexaferrite incorporation into the PU free-standing film made from fullerenol as a hypercross-linker, by varying its concentration from 1% to 5%.

EXPERIMENTAL

Materials

Fullerene C_{60} (CMer, 99.9%), hexamethylene diisocyanate (Acros Organics, Fair Lawn, NJ), dibutyltin dilaurate (Aldrich, St. Louis, MO), nano-$BaFe_{12}O_{19}$ (BaFe), and Triton X-114 were procured from Sigma Aldrich (St. Louis, MO). Polytetramethylene glycol (M_w = 2000) was dried in vacuum for 2 days to ensure complete removal of moisture. Methanol, dimethyl formamide, and tetrahydrofuran (THF) have been dried by known methods and stored over molecular sieves (4 Å) before use.

Synthesis of nano-BaFe-incorporated fullerene-containing PU flexible free-standing film

Synthesis of fullerenol $C_{60}(OH)_{12\text{-}13}$

Fullerenol was synthesized by Chiang et al.'s method.[25] All physical and spectroscopic data were in accordance with published results.

Synthesis of prepolymer

In a three-necked round-bottom flask, polytetramethylene glycol and hexamethylene diisocyanate (4 : 1 equiv.) were stirred at 70°C for 2 hr under nitrogen, and completion of the reaction was confirmed by the appearance of urethanic carbonyl at 1720 cm^{-1} in infrared (IR) spectrum.

Synthesis of nano-BaFe-incorporated C_{60}-PU nanocomposite

Synthesis of C_{60}-derived polymer network[26] was performed by adding C_{60}-OH_{12} (synthesized as earlier) and variable concentrations (1%, 2%, and 5%) of nano-BaFe sonicated in THF to prepolymer in anhydrous mixture of THF and dimethyl formamide (3 : 1) at 60°C under atmosphere pressure of N_2 in the presence of a dilute drop of dibutyltin dilaurate catalyst. Triton X 0.01 wt % was used for dispersion of BaFe. The viscosity began to increase, and, at an appropriate viscosity, the flexible free-standing films were casted by spin coating or doctor blade film applicator.

Characterization

Fourier transform infrared (FTIR) spectra were recorded on a Nicolet Magna IR 750 spectrometer, using KBr pellets. Thermogravimetric measurements were made with a TA instrument using a Hi-Res TGA 2950 thermogravimetric analyzer (TA Instruments, New Castle, DE) attached to a thermal analyst 2100 (DuPont Instruments, Newton, CT) thermal analyzer, at a heating rate of 10°C/min under nitrogen atmosphere. About 7 ± 2 mg of sample was heated at 10°C/min from room temperature to 1000°C in a dynamic nitrogen atmosphere (flow rate 60 mL/min). X-ray diffractograms (XRD) were recorded on an ARL XTRA X-ray diffractometer (Thermo Electron Corp., Waltham, MA) with Cu Kα radiation in the 2θ range from 10° to 80°, by a step of 0.02°. The particle size distribution and morphology was determined by Carl-Zeiss scanning electron microscope operated at high magnification, and energy-dispersive X-ray (EDX) spectrogram was recorded on Genesis 1000 attached with scanning electron microscope. The size and morphology of nanoferrite in the composite was confirmed by Technai G^2 U-Twin high-resolution transmission electron microscope. Tensile properties of polymers were analyzed on Sintech Universal Mechanical Testing Unit (ASTM D638). The standard dumb-bell-shaped samples were used in measurement with a constant stretching rate of 50 ± 10 mm/min. The real and imaginary permittivity and permeability (ε′, ε″, μ′, and μ″) were measured by Agilent PNA Series vector network analyzer E8364B (110–50 MHz) at X band (8.2–12.4 GHz) of microwave region. The values were

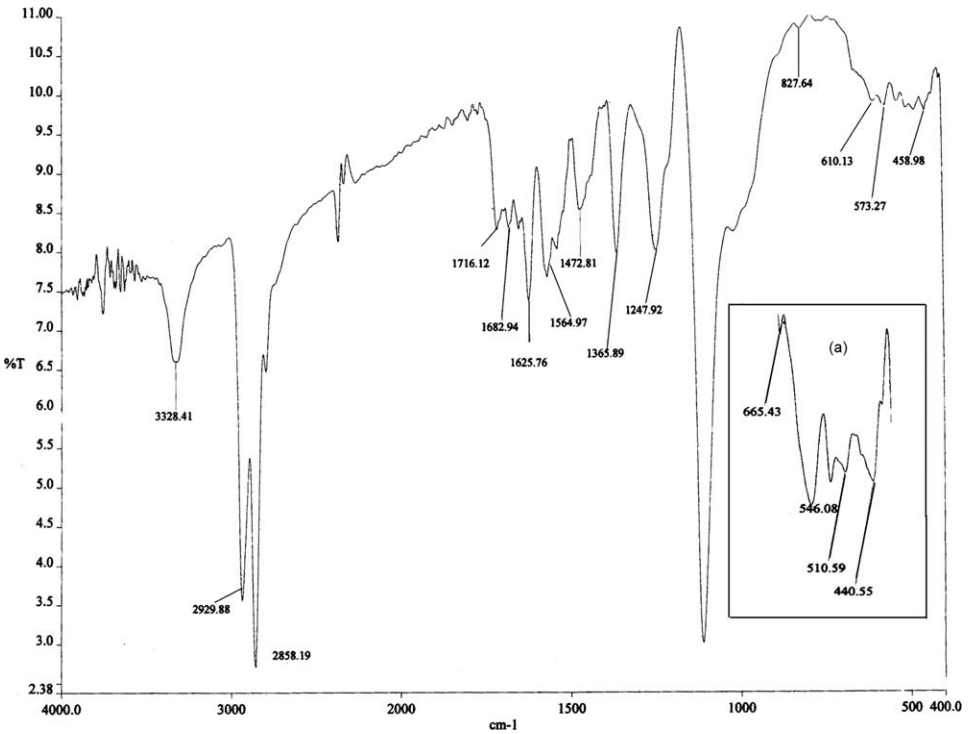

Figure 1 IR spectrum of BaFe-C_{60}-PU nanocomposite. Inset (a): IR of BaFe.

measured by Agilent X-Band (WR-90) waveguide kit using the material measurement software 85701.

RESULTS AND DISCUSSION

FTIR spectroscopy

The FTIR spectra of pure barium hexaferrite (BaFe) and its nanocomposites with PU are shown in Figure 1. The peaks at 592 and 440 cm^{-1} may be attributed to the intrinsic vibration of the tetrahedral and octahedral sites in the BaFe particles, respectively. The spectrum of the nanocomposite shows characteristic peaks of BaFe in addition to the urethanic N-H and carbonyl stretching at 3328 and 1716 cm^{-1}, respectively. These observations confirm the incorporation of the nanoparticles in the PU matrix.

X-ray diffraction

XRD of BaFe and its PU nanocomposite is shown in Figure 2(a,b). The diffraction peaks in Figure 2(a) are in accordance with the standard peaks for M-type hexagonal barium ferrite based on the JCPDS card 84-0757. The crystal size was calculated using the Scherrer equation:

$$d = k\lambda/\beta\cos\theta$$

where, d is the primary particle size, k is the Scherrer constant (0.889), λ is the wavelength of Cu Kα radiation (1.5405 Å), θ is the diffraction angle, and β is the full width half maxima of the peak. The average size of the sample calculated is 49 nm. The critical diameter of spherical barium ferrite with single magnetic domain is reported to be 460 nm.[27] Thus, all BaFe particles in this communication are of single domain. The XRD pattern in Figure 2(b) confirms the incorporation of BaFe because almost all characteristic peaks of BaFe at 30.3, 32.1, 34.1, 37, 40.3, 56.5, and 63 2θ are found to be present.

Morphology

The morphology and particle sizes of the samples were determined by scanning electron microscopy and transmission electron microscopy (TEM).

Scanning electron microscopy

Figure 3 shows the scanning electron microscopy image of BaFe-C_{60}-PU nanocomposite. The figure consists of microaggregates with ultrafine particles mostly of platelet shape in the size range of 50–100 nm. Some of the particles are aggregated, which may be attributed to their high surface energy. Their size is much below the critical diameter of barium hexaferrite (460 nm). For ferromagnetic particles smaller than Dc, the domain formation is no more energetically favored. Hence, all particles are expected to be single-domain particles.

Transmission electron microscopy

Figure 4(a) shows the TEM image of nano-BaFe. It can be observed from the image that most of the

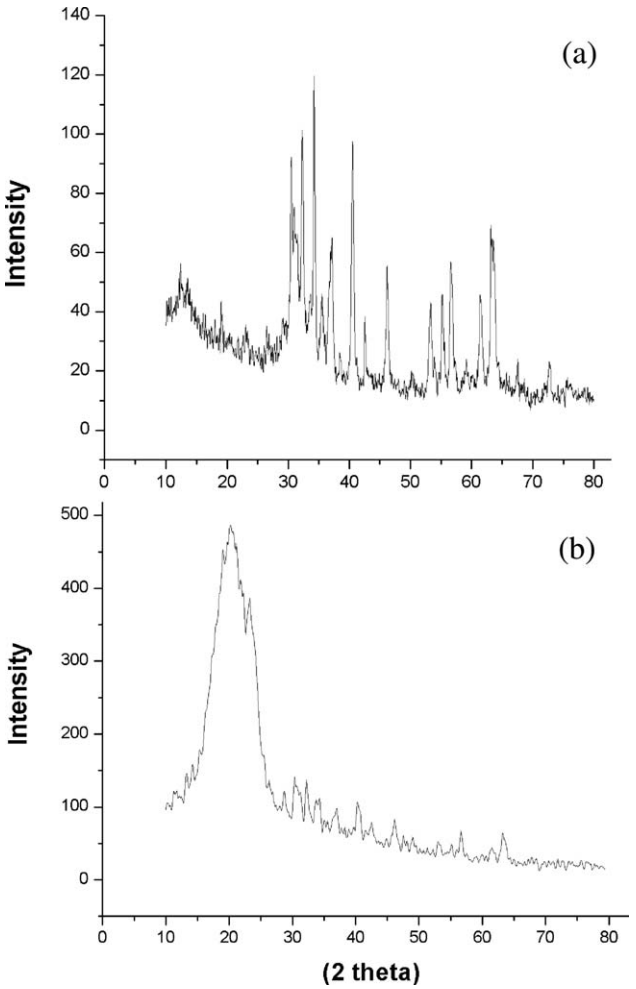

Figure 2 XRD spectrum of (a) BaFe and (b) BaFe-C_{60}-PU nanocomposite.

ferrite particles are hexagonal or spherical, with sizes in the range of 50–100 nm. These particles are polydisperse, and they stack each other because of the magnetic attraction between these particles. Figure 4(b) shows the TEM micrographs of BaFe-C_{60}-PU nanocomposite, which is quite polydispersed.

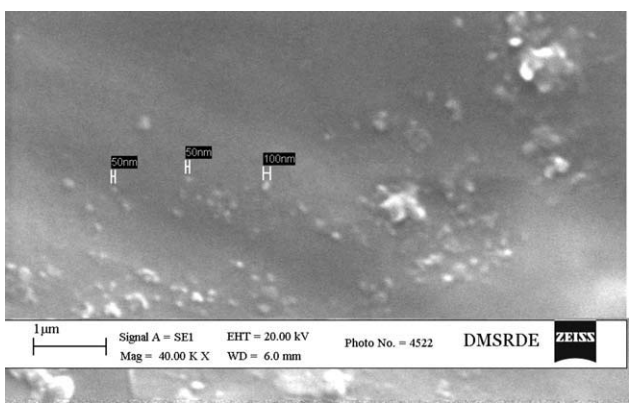

Figure 3 SEM micrograph of BaFe-C_{60}-PU nanocomposite.

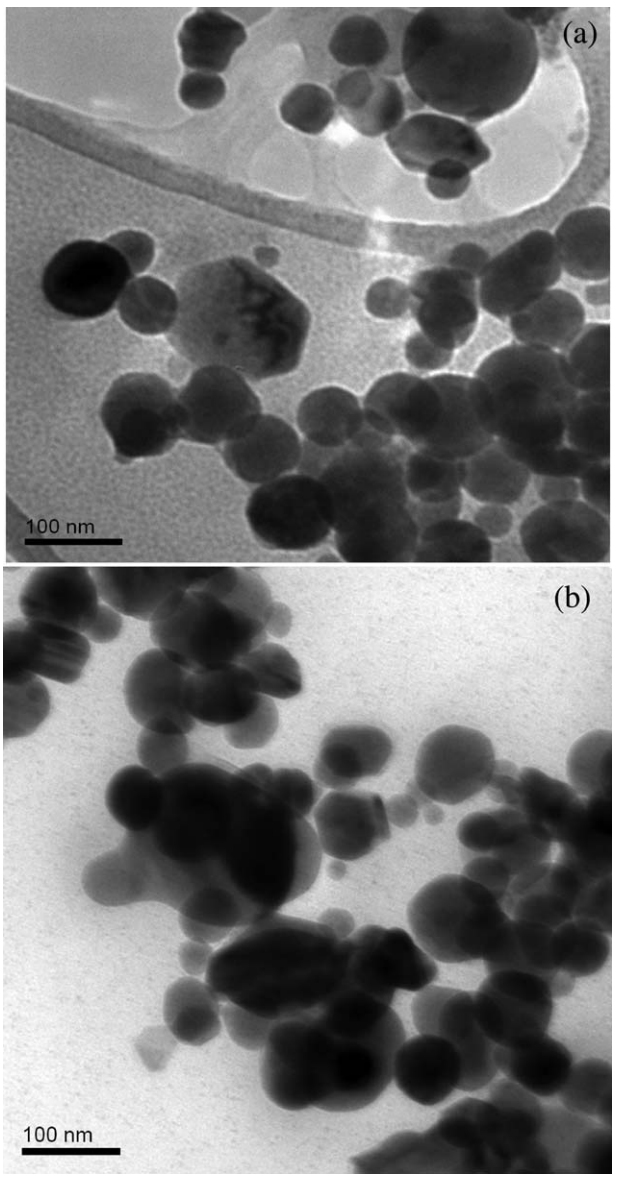

Figure 4 TEM micrograph of (a) BaFe and (b) BaFe-C_{60}-PU nanocomposite.

About 80–90% of the particles ranged from 50 to 100 nm, and the smaller spherical particles evident in the micrograph are probably of fullerene moiety.

Energy-dispersive X-ray diffraction

Figure 5(a,b) shows the EDX diffraction of nano-BaFe and its nanocomposite and provides another evidence for nano-BaFe incorporation into PU matrix. The elemental composition calculated from EDX (Table I) diffraction is in accordance with the expected values.

Thermal properties

The thermogravimetric analysis trace (Fig. 6) compares the thermal stability of nano-BaFe-incorporated PU with different BaFe ratios. As is evident

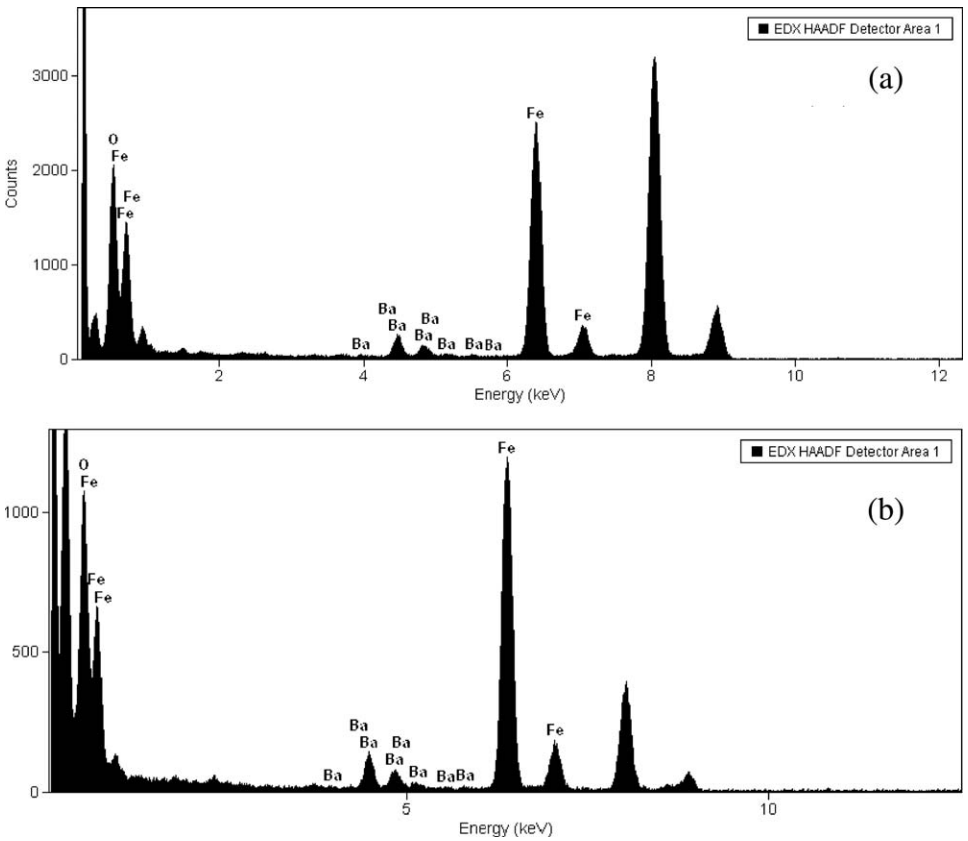

Figure 5 EDX of (a) BaFe and (b) BaFe-C_{60}-PU nanocomposite.

from the figure, there is no difference in the onset temperature for all the samples, but the increase in residual weight at 460°C as we move from 1% to 5% BaFe is another supportive evidence of its incorporation into the fullerene-containing PU films.

Mechanical properties

The enhancement in tensile strength with increasing concentration of the filler is expressed in Table II. Linear PU using butanediol as chain extender in place of fullerenol was also synthesized to compare its mechanical properties. This linear PU was found to possess very good elongation (900%), but the tensile strength was only 5 MPa. The fullerene-containing PU has tensile strength of 12 MPa,[28,29] and addition of 1–5% BaFe filler raises its tensile strength upto 34 MPa. Hence, the nanofiller impart remarkable mechanical strength to the nanocomposite.

TABLE I
EDX Elemental Composition of 5% BaFe-C_{60}-Polyurethane Nanocomposite

S. Name	Tensile strength (MPa)	% Elongation (E_b)
Fe-PU-1	23.7	731
Fe-PU-2	25.9	668
Fe-PU-5	34.7	900

Microwave absorbing properties

Figure 7 plots the real and imaginary parts of permeability (μ′ and μ″) of absorbing barium hexaferrite PU nanocomposite with different filler concentration. We can find from the figure that μ′, μ″, and loss factor (tan δμ) increase with the increasing concentration of BaFe in the frequency range of X band. As shown in Figure 7(c), the resonance peak for loss

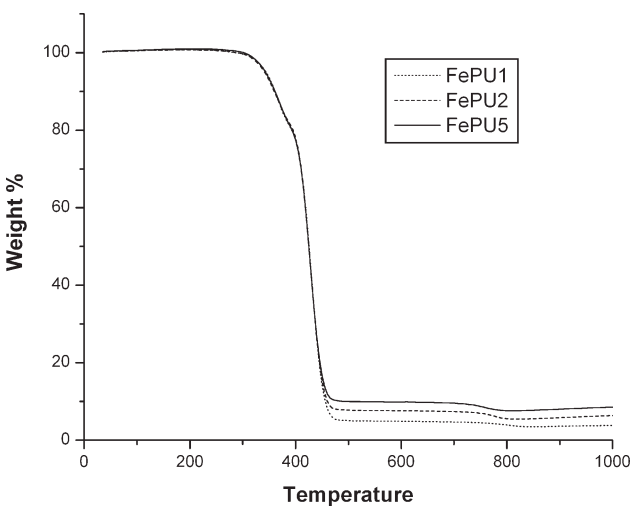

Figure 6 TGA thermograms of 1%, 2%, and 5% of BaFe-C_{60}-PU nanocomposites.

TABLE II
Tensile Properties of Barium Hexaferrite-C_{60}-Polyurethane Nanocomposites

% Comp.	BaFe	Fe-PU-5
C K	–	73.2
N K	–	9.1
O K	19.6	14.6
Ba L	12.9	0.67
Fe K	67.5	2.28

tangent curve for 1, 2, and 5% nanocomposite increases from 0.19 at 8.7 GHz, to 0.22 at 8.7 GHz, and to 0.39 at 8.8 GHz, respectively. The increase in loss factor may be attributed to magnetic dissipation through hysteresis loss, ferromagnetic resonance loss, intragranular domain wall loss, etc. It is well known that barium ferrite particles possess high coercive force and hysteresis loop area[30] and, collectively, these two factors may lead to larger magnetic hysteresis loss. Although at high frequencies, ferromagnetic resonance occurrence is the basic phenomenon used to absorb microwave radiation, when the external microwave frequency is equal to or more than the frequency of ferromagnetic resonance, barium will absorb plenty of energy to support the domain rotation. Ferromagnetic resonance is the primary channel of barium ferrite to absorb energy in the microwave band, and it accords with the maximum loss on the microwave loss spectra.[31]

Figure 8 plots the real and imaginary parts of permittivity (ε' and ε'') of the nanocomposites with different filler concentration. Figure 8(b) clearly shows the increase in ε'' from 0.32 to 0.36 with increase in the filler concentration from 1% to 5% at 10.3 GHz. This expected increase of ε'' and tan δ_ε with increase in filler content suggests the enhancement in lossy characteristic of the nanocomposite.

The reflection loss was calculated from measured data using theory of the absorbing wall for different ferrite to PU ratios. According to transmission line theory, the reflection loss of a microwave absorbing layer backed by a perfect conductor was calculated by the following equations:

$$RL(\mathrm{dB}) = 20\log\left|\frac{Z_{\mathrm{in}} - Z_{\mathrm{o}}}{Z_{\mathrm{in}} + Z_{\mathrm{o}}}\right| \quad (1)$$

$$Z_{\mathrm{o}} = \sqrt{\frac{\mu_{\mathrm{o}}}{\varepsilon_{\mathrm{o}}}} \quad (2)$$

$$Z_{\mathrm{in}} = \sqrt{\frac{\mu_r}{\varepsilon_r}}\tanh\left[j\frac{2\pi fd}{c}\sqrt{\mu_r\varepsilon_r}\right] \quad (3)$$

where RL is a ratio of reflected power to incident power in dB, Z_0 is the characteristic impedance of free space, Z_{in} is the normalized input impedance relative to the impedance in free space, $\varepsilon_r = \varepsilon' - j\varepsilon''$ and $\mu_r = \mu' - j\mu''$ are the complex permittivity and complex permeability of the composite medium, respectively, d is the thickness of the absorber, and c and f are the velocity of light and the frequency of microwave in free space, respectively. The impedance matching condition is given by $Z_{\mathrm{in}} = Z_0$ to represent the perfect absorbing properties.

The microwave reflection loss values were measured for the BaFe-C_{60}-PU nanocomposite films having thicknesses of 2 and 3 mm. The reflection losses of composites as a function of frequency for all the samples are shown in Figure 9. As shown in Figure 9(b), FePU-1 shows a maximum reflection loss of −3.5 dB at 8.6 GHz, FePU-2 shows −4.7 dB at

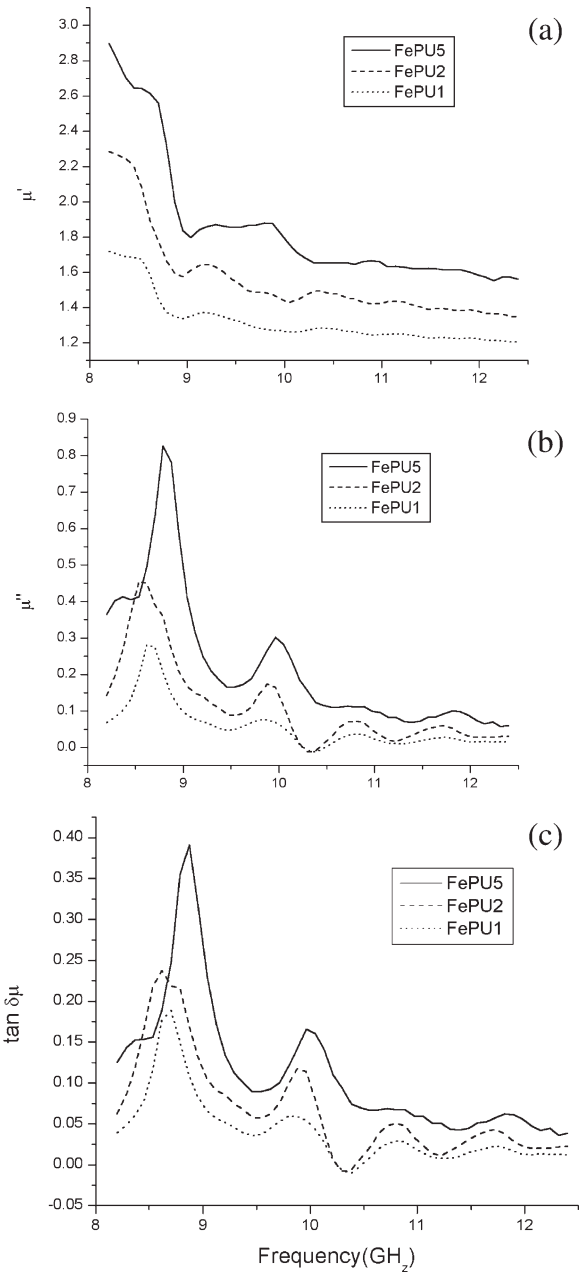

Figure 7 Plot of (a) real permeability (μ'), (b) imaginary permeability (μ''), and (c) tan δ_μ versus frequency of 1%, 2%, and 5% BaFe-C_{60}-PU nanocomposites.

8.6 GHz, and FePU-5 −7.5 dB at 8.8 GHz. The maximum reflection loss increases from −3.7 to −7.5 dB for 3-mm nanocomposite. Figure 9 also indicates that the position of maximum reflection loss peaks shifts to a higher frequency value with increasing ferrite content. The enhanced microwave properties may be attributed to the nanometer size of the particles, which provide large surface area and increased number of dangling bond atoms and unsaturated coordination on the surface. These variations lead to the interface polarization and multiple scatter, which is useful to absorb more microwave.

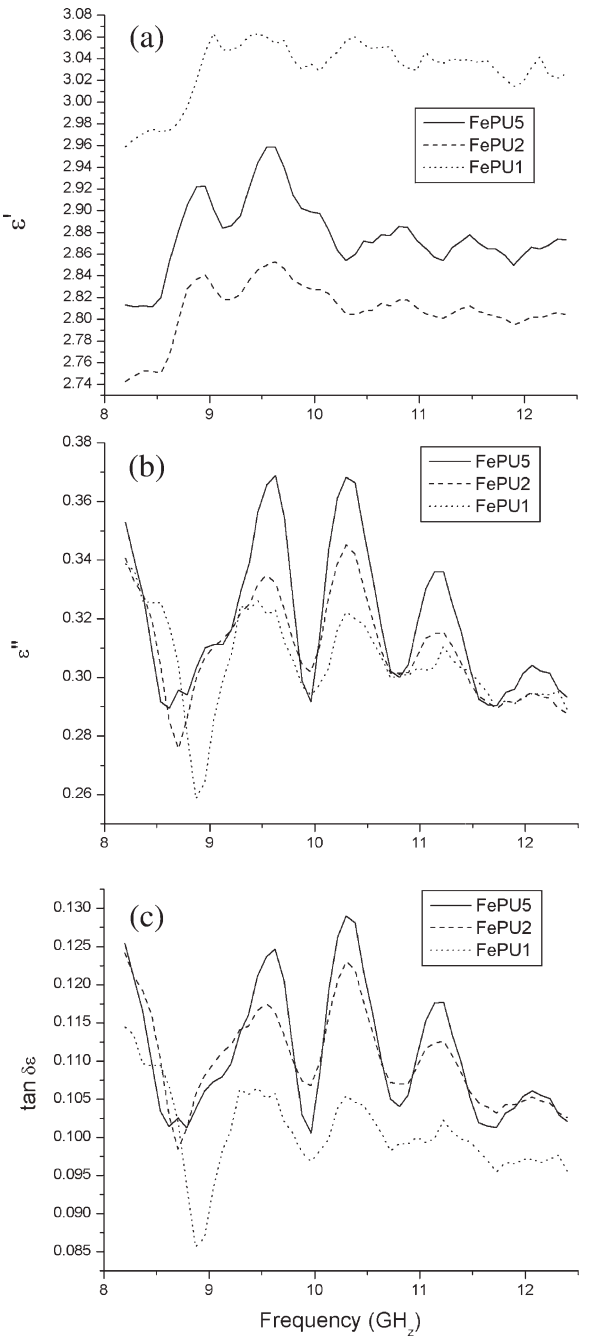

Figure 8 Plot of (a) real permittivity (ε′), (b) imaginary permittivity (ε″), and (c) tan δ_ε versus frequency of 1%, 2%, and 5% BaFe-C_{60}-PU nanocomposites.

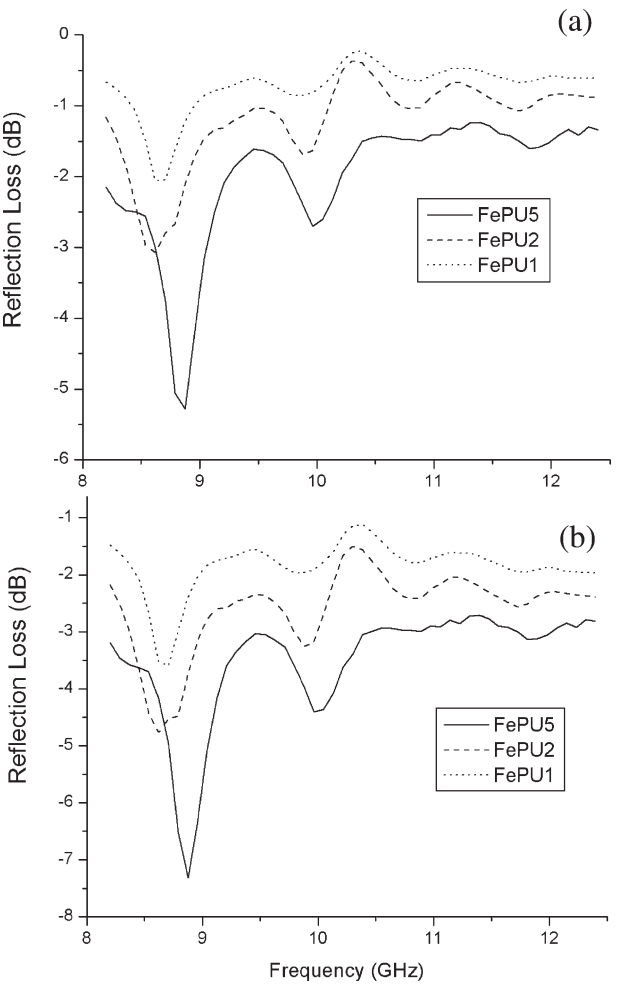

Figure 9 Plot of reflection loss versus frequency of (a) 2 mm and (b) 3 mm thickness of BaFe-C_{60}-PU nanocomposites.

CONCLUSIONS

In this communication, the novel nanocomposites of fullerene-containing PU and barium hexaferrite have been obtained. Their microstructure, morphology, and thermal, microwave, and electromagnetic properties have been studied. The complex permeability and permittivity were measured in the frequency range of 8.2–12.4 GHz. The maximum reflection loss of the nanocomposites was found to increase with increasing the ferrite content from 1% to 5%, with maximum value of −7.5 dB at only 5% composition. The films show homogeneous dispersion of ferrite particles and good magnetic properties for potential application as microwave absorbers.

The authors thank the Central Analytical Facility, DMSRDE, for providing scanning electron microscopy and EDX facility and TEM facility at IIT Kanpur.

References

1. Kun, J.-B.; Lee, S.-K.; Kum, C.-G. Comp Sci Technol 2008, 68, 2909.
2. Cho, S. B.; Kang, D. H.; Oh, J. H. J Mater Sci 1996, 31, 4719.
3. Babbar, V. K.; Razdan, A.; Puri, R. K.; Goel, T. C. J Appl Phys 2000, 87, 4362.
4. Ruan, S.; Xu, B.; Suo, H.; Wu, F.; Xiang, S.; Zhao, M. J Magn Magn Mater 2000, 212, 175.
5. Peng, C. H.; Wang, H.-W.; Kan, S.-W.; Shen, M.-Z.; Wei, Y.-M.; Chen, S.-Y. J Magn Magn Mater 2004, 284, 113.
6. Snoek, J. L. Physica 1948, 14, 207.
7. Wohlfarth, E. P. Ferromagnetic Materials, Vol. 3; North-Holland: New York, 1982.
8. Wang, S.; Ng, W. K.; Ding, J. Scr Mater 2000, 42, 861.
9. Surig, C.; Hempel, K. A.; Bonnenberg, D. Appl Phys Lett 1993, 63, 2836.
10. Radwan, M.; Rashad, M. M.; Hassien, M. M. J Mater Process Technol 2007, 181, 106.
11. Mu, G.; Chen, N.; Pan, X.; Shen, H.; Gu, M. Mater Lett 2008, 62, 840.
12. Kim, D. Y.; Chung, D. C.; Kang, T. W.; Kim, H. C. IEEE Trans Magn 1996, 32, 555.
13. Bean, C. P.; Livingston, J. D. J Appl Phys 1959, 30, 120S.
14. Kneller, E. F.; Luborsky, F. E. J Appl Phys 1963, 34, 656.
15. Tang, X.; Hu, K.-A. Mater Sci Eng B 2007, 139, 119.
16. Ghasemi, A.; Sepelak, V.; Liu, X.; Morisako, A. IEEE Trans Magn 2009, 45, 2456.
17. Park, K.-Y.; Han, J.-H.; Lee, S.-B.; Kim, J.-B.; Yi, J.-W.; Lee, S.-K. Compos Sci Technol 2009, 69, 1271.
18. Peng, C.-H.; Hwang, C.-C.; Wan, J.; Tsai, J.-S.; Chen, S.-Y. Mater Sci Eng B 2005, 117, 27.
19. Ohlan, A.; Singh, K.; Chandra, A.; Dhawan, S. K. Appl Mater Interface 2010, 2, 927.
20. Sugimoto, H.; Daimatsu, K.; Nakanishi, E.; Ogasawara, Y.; Yasumura, T.; Inomata, K. Polymer 2006, 47, 3754.
21. Dwivedi, M.; Alam, S.; Verma, G. L. Polym Int 2005, 54, 401.
22. Dwivedi, M.; Alam, S.; Verma, G. L. J Therm Anal Calorim 2005, 77, 947.
23. Dwivedi, M.; Alam, S.; Verma, G. L. Polym Plast Technol Eng 2005, 44, 1235.
24. Chopra, S.; Mathur, S.; Alam, S. J Polym Mater 2008, 25, 275.
25. Chiang, L. Y.; Wang, L.-Y.; Swirczewski, J. W.; Soled, S.; Cameron, S. J Org Chem 1994, 59, 3960.
26. Chiang, L. Y.; Wang, L.-Y.; Tseng, S.-M.; Wu, J.-S.; Hsieh, K.-H. J Chem Soc Chem Commun 1994, 2675.
27. Rezlescu, L.; Rezlescu, E.; Popa, P. D.; Rezlescu, N. J Magn Magn Mater 1999, 193, 288.
28. Wang, L.-Y.; Wu, J.-S.; Iseng, S.-M.; Kuo, C.-S.; Hsieh, K.-H.; Liau, W. B.; Chiang, L.-Y. J Polym Res 1996, 3, 1.
29. Chiang, L.-Y.; Wang, L.-Y.; Kuo, C.-S. Macromolecules 1995, 28, 7574.
30. Xu, P.; Han, X. J.; Wang, X. H.; Wang, C.; Zhao, H. T.; Zhang, W. J. Mater Chem Phys 2008, 108, 196.
31. Gairola, S. P.; Verma, V.; Singh, A.; Purohit, L. P.; Kotnala, R. K. Solid State Commun 2010, 150, 147.